

# A long side chain imidazolium-based graft-type anion exchange membrane: Novel electrolyte and alkaline durable properties and the structural elucidation using SANS contrast variation

Yue Zhao,<sup>1,\*</sup> Kimio Yoshimura,<sup>1</sup> Ahmed Mohamed Ahmed Mahmoud,<sup>1</sup> Hwan-Chul Yu,<sup>1</sup>  
Shun Okushima,<sup>1</sup> Akihiro Hiroki,<sup>1</sup> Yoshihiro Kishiyama,<sup>2</sup> Hideyuki Shishitani,<sup>2</sup> Susumu Yamaguchi,<sup>2</sup> Hirohisa Tanaka,<sup>3</sup> Yohei Noda,<sup>4</sup> Satoshi Koizumi,<sup>4</sup> Aurel Radulescu,<sup>5</sup> Yasunari Maekawa<sup>1,\*</sup>

**S1. Determination of  $\phi_{nc-graft}$  and  $\phi_{c-graft}$ .** Same as we reported in ref. 20, a specific matching point exists in the 2-phase system to make the scattering intensity minimum, at which the scattering length density (SLD) of phase 1 ( $b_1$ ) is close to that of phase 2 ( $b_2$ ), namely,  $b_1 \approx b_2$ . This criterion allows us to determine the distribution of graft polymer in phases 1 and 2 in a quantitative manner. To search the matching point, the evolution of  $I(q_1)^{1/2}$  with the volume fraction of D<sub>2</sub>O in the water mixture,  $f_{D_2O}$ , is presented in Figure S5. The volume fraction of D<sub>2</sub>O at the matching point ( $f_{D_2O,m}$ ) was determined from the minimum value of  $I(q_1)^{1/2}$  to be about 70%, 60%, and 56% for AEM14, AEM42, AEM86, respectively.

Obviously,  $\phi_{nc-graft}$  and  $\phi_{c-graft}$  also satisfy Eq. (S1) below:

$$\phi_{nc-graft} + \phi_{c-graft} = \phi_{graft} \quad (S1)$$

It is worthy to note that the SLD of the non-conducting phase ( $b_1$ ) is a constant, being independent of  $f_{D_2O}$  due to the strong immiscibility with water. The SLD of the conducting phase ( $b_2$ ), however, varies with the incorporated water.  $b_1$  or  $b_2$  can be given in terms of  $\phi_{nc-graft}$  and  $\phi_{c-graft}$  as shown in the following equations:

$$b_1 = \frac{\phi_{nc-graft} b_{graft} + \phi_{ETFE} b_{ETFE}}{\phi_{nc-graft} + \phi_{ETFE}} \quad (S2)$$

$$b_2 = \frac{\phi_{c-graft} b_{graft} + \phi_w b_w}{\phi_{c-graft} + \phi_w} \quad (S3)$$

where  $b_x$  (X= graft, ETFE or w, represents graft polymer, ETFE or water, respectively) means the SLD of X, which can be calculated theoretically according to the molecular structure and the mass density of X.<sup>20</sup> Thus  $b_{graft} = 1.07 \times 10^{10} \text{ cm}^{-2}$ . The exact mass density of either ETFE crystalline or amorphous chain is unknown; however, plenty of previous reports showed that the scattering intensity of the neat ETFE base films is very weak, suggesting a negligible small difference in the SLD of ETFE crystalline and amorphous domains.<sup>14, 16, 20</sup> Therefore, it is reasonable to use the average mass density of ETFE film of  $\sim 1.7 \text{ g/cm}^3$  to roughly estimate the SLD of ETFE crystalline and amorphous domains to be  $\sim 2.7 \times 10^{10} \text{ cm}^{-2}$ .  $b_w$  is a function of  $f_{D2O}$  given by

$$b_w = b_{D2O} f_{D2O} + b_{H2O} (1 - f_{D2O}) \quad (S4)$$

where  $b_{D2O}$  and  $b_{H2O}$  are the SLD of D<sub>2</sub>O and H<sub>2</sub>O being 6.34 and -0.56 ( $\times 10^{10} \text{ cm}^{-2}$ ), respectively.<sup>36</sup>

At the matching point of  $f_{D2O,m}$ , Eqs. (S2) and (S3) were equivalent to each other. In conjunction with Eq. (S1), we can accurately estimate  $\phi_{nc-graft}$  and  $\phi_{c-graft}$  for each AEM as listed in Table 2.

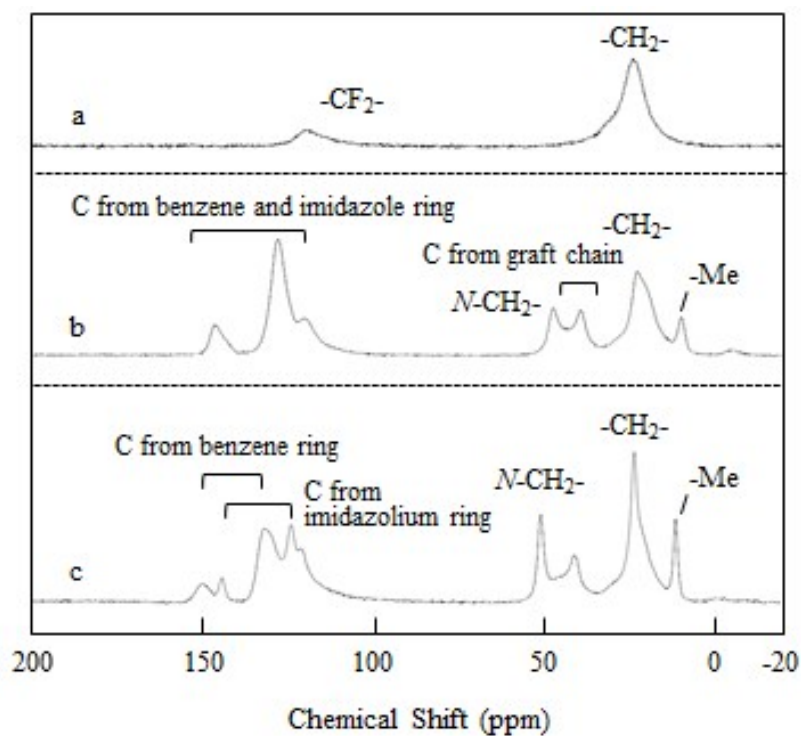


Figure S1  $^{13}\text{C}$  solid-state NMR spectrum of (a) ETFE, (b) poly(StIm)-grafted ETFE with a grafting degree of 46%, (c) StIm-AEM with a grafting degree of 50% in  $\text{Cl}^-$  form.

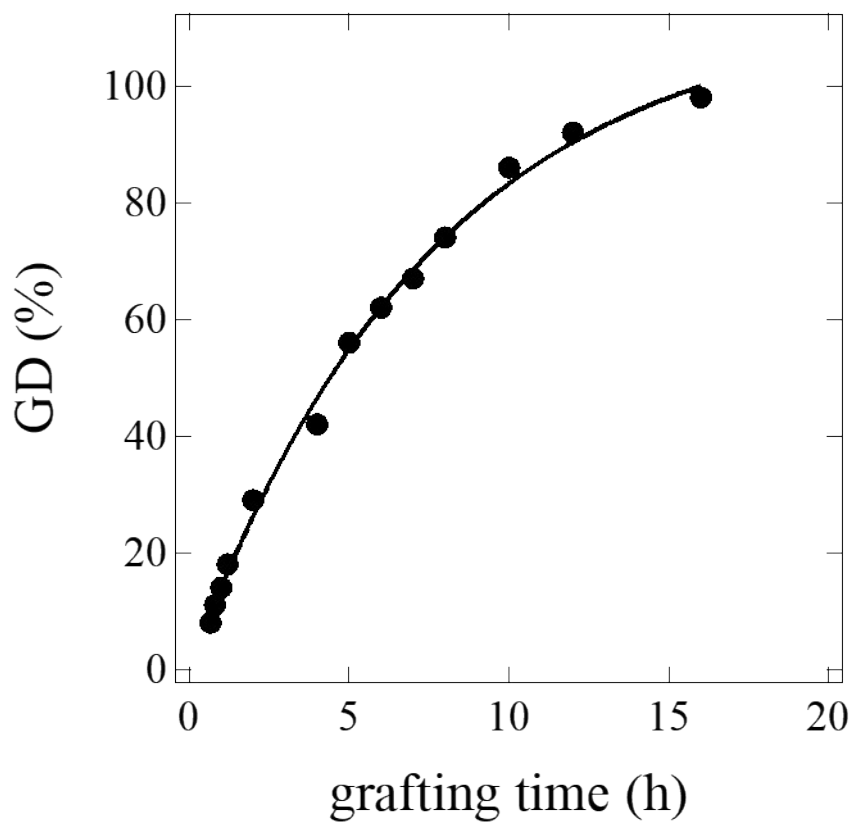


Figure S2 Plot of GD as a function of grafting polymerization time

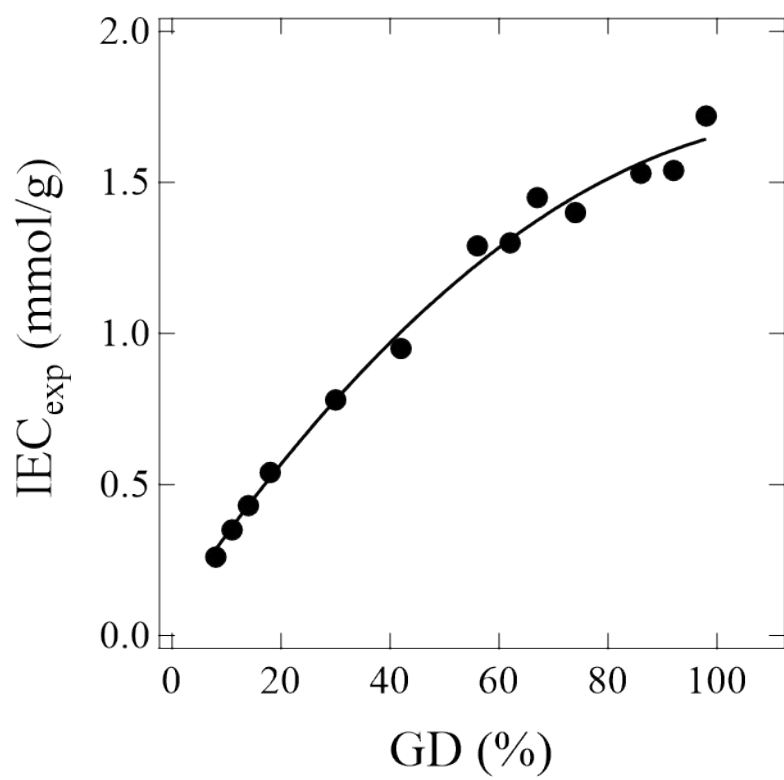


Figure S3 Plot of effective IEC<sub>exp</sub> as a function of GD.

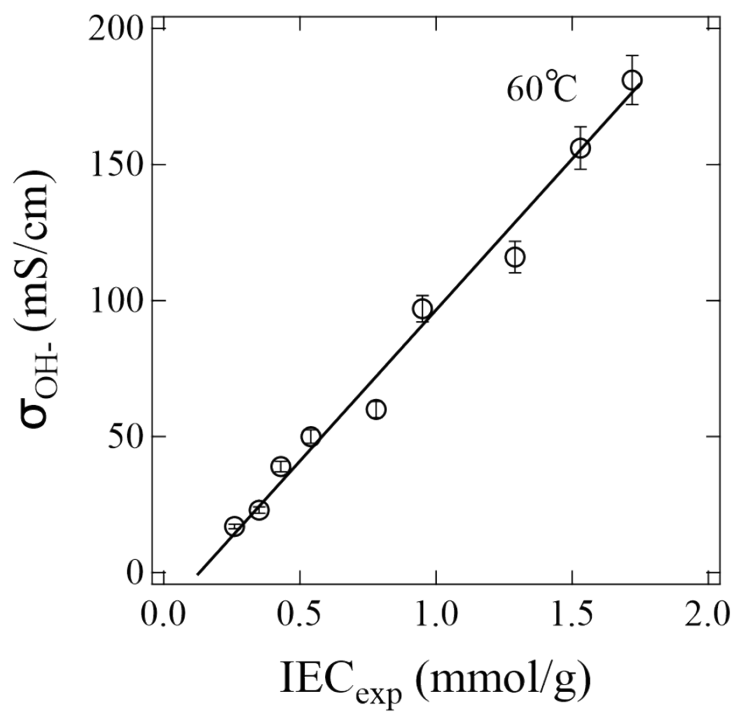


Figure S4 Plot of  $\sigma_{\text{OH}^-}$  at 60 °C as a function of IEC<sub>exp</sub>.

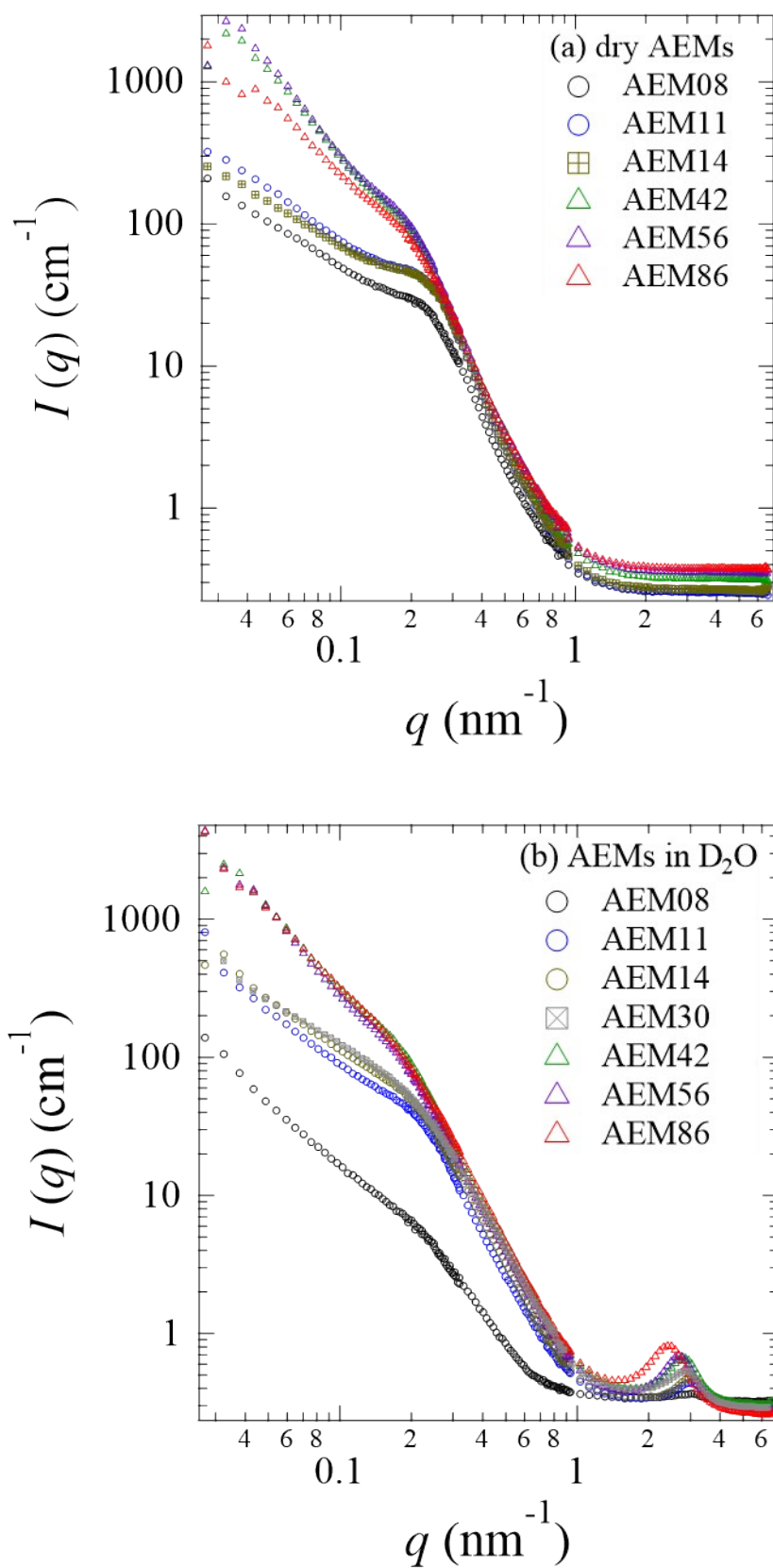


Figure S5 SANS intensity profiles of (a) dry AEMs and (b) AEMs equilibrated in D<sub>2</sub>O, with different GDs equilibrated in D<sub>2</sub>O before incoherent scattering correction.





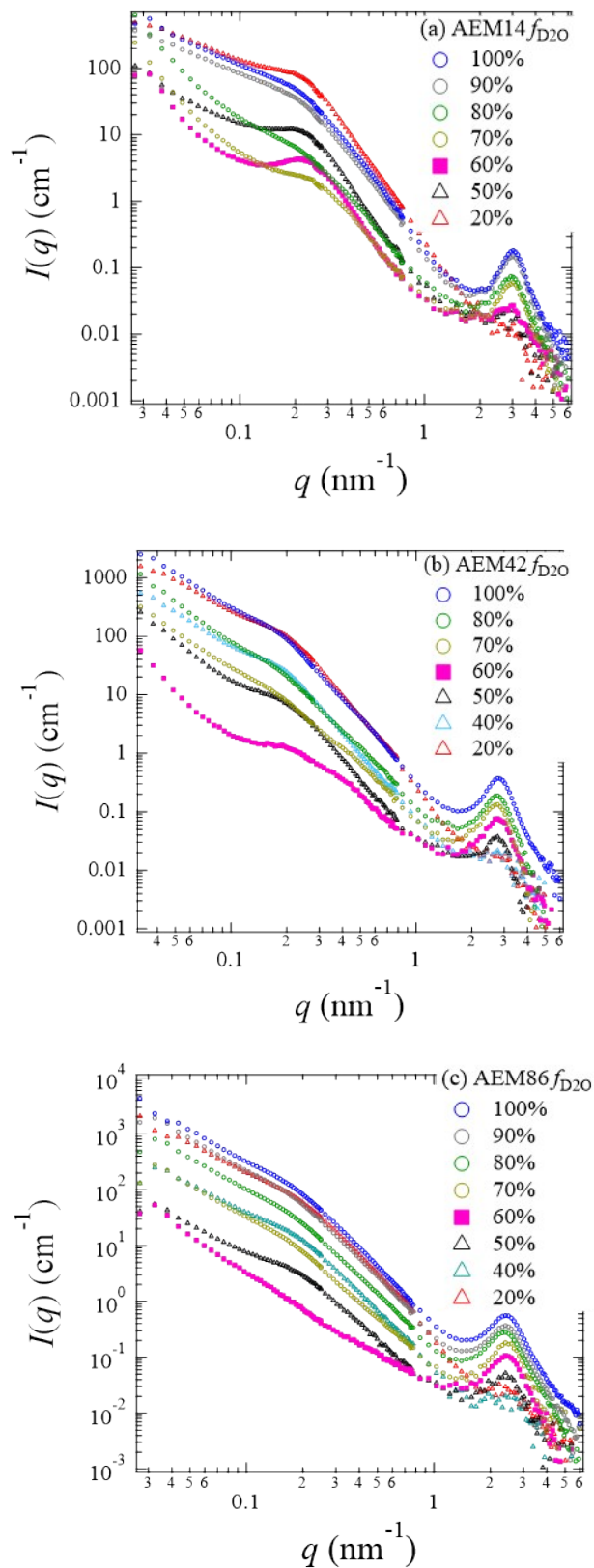


Figure S6 SANS profiles obtained from (a) AEM14; (b) AEM42; and (c) AEM86 equilibrated in water mixture with different representative  $f_{\text{D}_2\text{O}}$ .

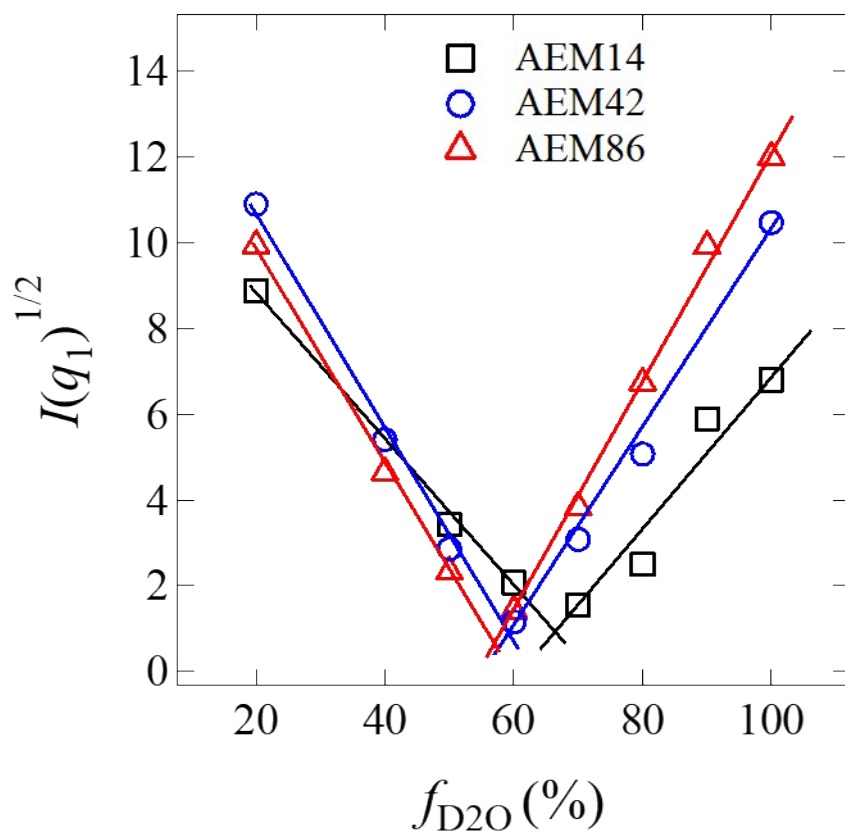


Figure S7 The volume fraction  $f_{D2O}$  dependence of  $I(q_1)^{1/2}$  observed for AEMs equilibrated in  $H_2O/D_2O$  water mixtures shown in Figure S4.

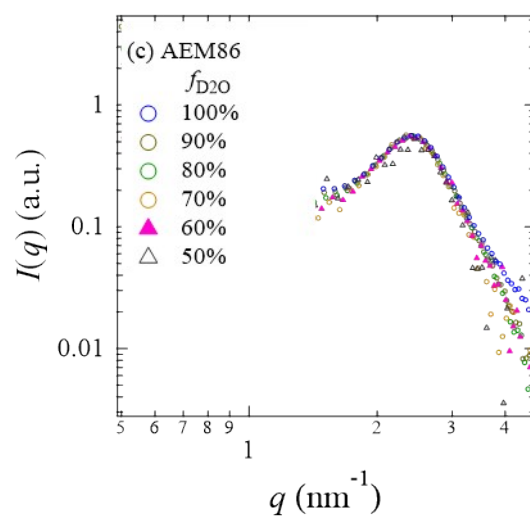
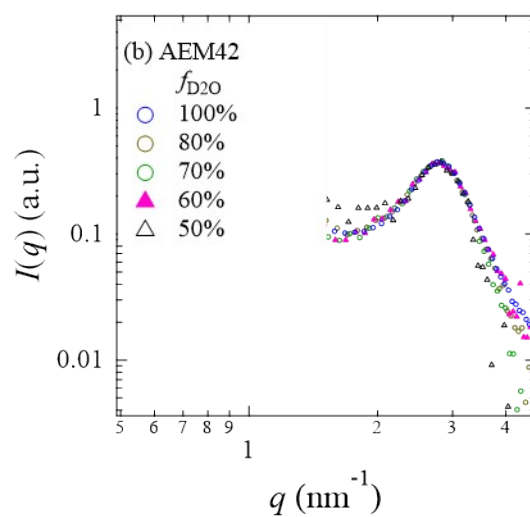
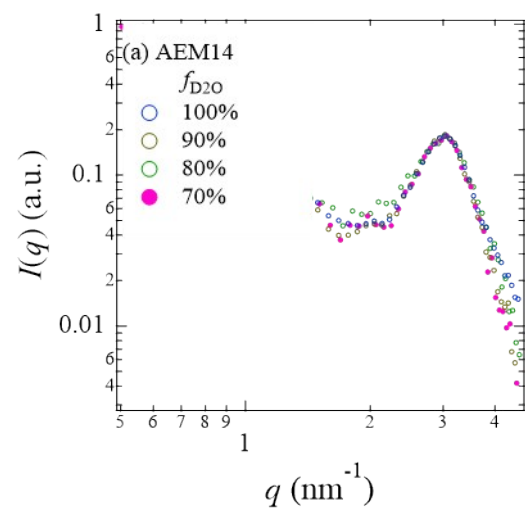


Figure S8 Vertically shifted SANS profiles around the ionomer peak for (a) AEM14; (b) AEM42; and (c) AEM86 equilibrated in  $\text{H}_2\text{O}/\text{D}_2\text{O}$  water mixtures with representative  $f_{D_2O}$ .

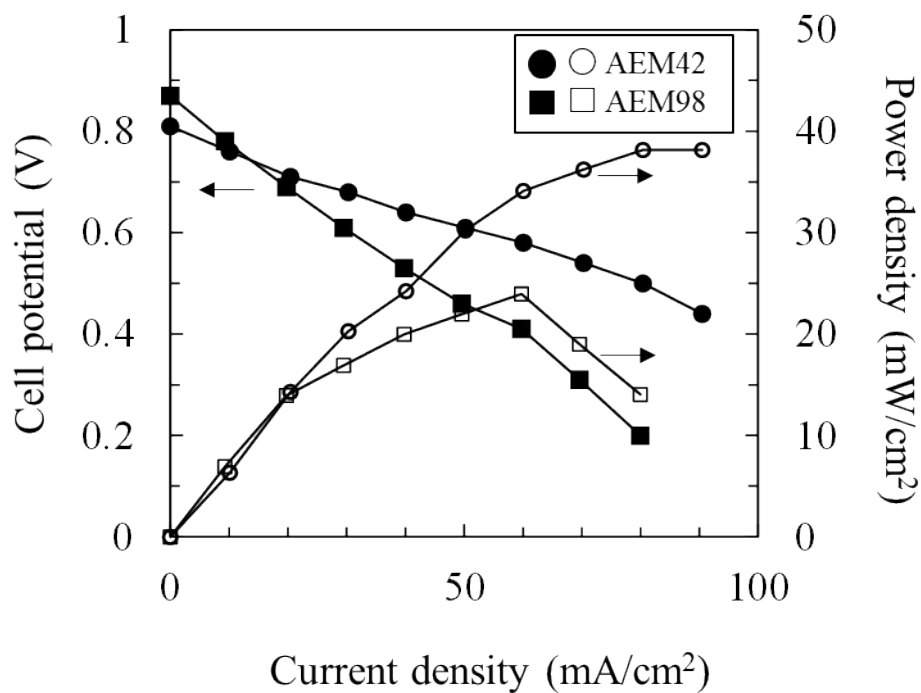


Figure S9 Polarization curve and power density of the single hydrazine hydrate fuel cell fabricated with AEM42 or AEM98 as a membrane, and BTMA as an ionomer at 80°C, 50 mL/min oxygen flow rate, and 20 mL/min hydrazine hydrate with 10 KPa backpressure at the cathode side.